

1 Evidence for an exceptional 20th-Century slowdown in Atlantic Ocean 2 overturning

3
4 Stefan Rahmstorf*, Jason Box, Georg Feulner, Michael E. Mann, Alexander Robinson, Scott Rutherford and Erik
5 Schaffernicht

6 **Possible changes in Atlantic meridional overturning circulation (AMOC) provide a key source of**
7 **uncertainty regarding future climate change. Maps of temperature trends over the 20th Century**
8 **show a conspicuous region of cooling in the northern Atlantic. Here we present multiple lines of**
9 **evidence suggesting that this cooling may be due to a reduction in the AMOC over the 20th Century**
10 **and particularly after 1970. Since 1990 the AMOC appears to have partly recovered. This time**
11 **evolution is consistently suggested by an AMOC index based on surface temperatures, by the**
12 **hemispheric temperature difference, by coral-based proxies and by oceanic measurements. We**
13 **discuss a possible contribution of the melting of the Greenland Ice Sheet to the slowdown. Using a**
14 **multi-proxy temperature reconstruction for the AMOC index suggests that the AMOC weakness**
15 **after 1975 is an unprecedented event in the past millennium ($p > 0.99$). Further melting of**
16 **Greenland in the coming decades could contribute to further weakening of the AMOC.**

17 Global warming during the 20th Century has not proceeded uniformly over the globe. A small portion
18 of the Earth's surface has even cooled since the start of the 20th Century: a region over the subpolar
19 gyre of the North Atlantic, to the south of Greenland (Fig. 1). Model simulations show the largest
20 cooling response to a weakening of the Atlantic meridional overturning circulation (AMOC) in this
21 same region¹, suggesting this area has so far defied global warming due to a weakening of the AMOC
22 over the past century. The time history of the AMOC over this period is poorly known, however, due
23 to the scarcity of direct measurements. Because of the large heat transport associated with the
24 AMOC, changes in sea surface temperatures (SSTs) can be used as an indirect indicator of the AMOC
25 evolution².

26 Dima and Lohmann³ identified two distinct modes in global SST evolution, one associated with a
27 gradual decline of the global thermohaline circulation and one due to multidecadal and shorter
28 AMOC variability, and concluded "that the global conveyor has been weakening since the late 1930s
29 and that the North Atlantic overturning cell suffered an abrupt shift around 1970". Thompson et al.⁴
30 found that the SST difference between the Northern and Southern Hemisphere underwent a sudden
31 decline by ~0.5 °C around 1970, with the largest cooling observed over the northern Atlantic. We

32 interpret this as indicative of a large-scale AMOC reduction, since the most plausible explanation for
33 such a rapid change in the interhemispheric temperature difference is the cross-equatorial heat
34 transport of the AMOC⁵. Drijfhout et al.⁶ regressed the AMOC strength and global-mean
35 temperature on surface temperature fields in models and concluded that the conspicuous “warming
36 hole” south of Greenland is related to a weakening of the AMOC. They further found that a possible
37 contribution of aerosol forcing to the cool patch as proposed by Booth et al.⁷ cannot be excluded.

38 Zhang et al.⁸, however, argue that the model simulation by Booth et al. overestimates the effect of
39 aerosol forcing, by not accounting for any increase in ocean heat content in the North Atlantic over
40 the second half of the 20th Century, in contrast to what is suggested by the observations. The
41 observational data show a clear dipole response in the Atlantic, with the North Atlantic cooling and
42 the South Atlantic warming when comparing 1961-1980 with 1941-1960. The maximum of South
43 Atlantic warming is within the Benguela Current off southern Africa and the maximum of North
44 Atlantic cooling is found within the Gulf Stream. These patterns are highly characteristic of AMOC
45 changes and are found in many model simulations wherein the AMOC is weakened by freshwater
46 hosing experiments. The Atlantic see-saw pattern can also be seen in Fig. 1, where out of all
47 Southern Hemisphere ocean regions the South Atlantic has warmed the most.

48 Terray⁹ has analysed the current CMIP5 ensemble of model simulations together with observed SST
49 data in order to quantify the relative contributions of radiatively forced changes to the total decadal
50 SST variability. While in most models forced changes explain more than half of the variance in low
51 latitudes, they explain less than 10% in the subpolar North Atlantic, where in most cases their
52 contribution is not significantly different from zero (the notable exception is the model used by
53 Booth et al. as mentioned above).

54 In order to put the 20th Century AMOC evolution into a longer-term context, in the following we
55 develop an AMOC index based on surface temperatures from instrumental and proxy data.

56 **An AMOC index based on surface temperatures**

57 We take the results of a climate model intercomparison¹ to identify the geographic region that is
58 most sensitive to a reduction in the AMOC (Fig. 1), which for simplicity we henceforth refer to as
59 ‘subpolar gyre’, although we use the term here merely to describe a geographic region and not an
60 ocean circulation feature. To isolate the effect of AMOC changes from other climate change, we
61 define an AMOC index by subtracting the Northern Hemisphere mean surface temperature from
62 that of the subpolar gyre (see *Supplementary Information* for an alternative index obtained by
63 subtracting Northern Hemisphere SST). We thus assume that differences in surface temperature

64 evolution between the subpolar gyre and the whole Northern Hemisphere are largely due to
65 changes in the AMOC. This appears to be a reasonable approximation in view of the evidence on
66 North Atlantic SST variability discussed in the introduction. We decided against using an index based
67 on a dipole between North and South Atlantic temperatures^{2, 10}, as this might be affected by the
68 large gradient in aerosol forcing between both hemispheres.

69 We test the performance of the index in a global warming scenario experiment for 1850-2100 with a
70 state-of-the-art global climate model, the MPI-ESM-MR. This model has a realistic representation of
71 the AMOC^{10, 11} based on criteria that include the magnitude and shape of the AMOC stream function
72 and the realism of sites of deep-water formation. Without satisfying those criteria, we cannot expect
73 realistic spatial patterns of SST response to AMOC variations and hence a good correlation of our
74 temperature-based AMOC index with the actual AMOC. An analysis of 10 global climate models
75 found that a surface temperature response in the North Atlantic subpolar gyre is a robust feature of
76 AMOC variability, while the details of this response depend on the quality of representation of the
77 AMOC¹⁰.

78 Fig. 2 shows a high correlation of the AMOC index with the actual AMOC in the model, particularly
79 on time scales of a decade and longer (smoothed curves). The correlation coefficient of the two
80 smoothed curves after linear detrending is $R=0.90$ and our temperature-based AMOC index predicts
81 the actual AMOC changes in the model with an RMS error of 0.6 Sv (1.1 Sv for the annual data),
82 where the conversion factor of 2.3 Sv/K has been fitted. Note that both individual components of
83 the index – the subpolar gyre and the Northern Hemisphere temperature – increase during the 21st
84 Century in the simulation; it is the difference between the two which tracks the AMOC decline, as
85 expected by our physical understanding of the effect of AMOC heat transport.

86 The lower panel of Fig. 2 shows the correlation pattern of the AMOC stream function in the model
87 with our AMOC index, which displays coherent large-scale structure that resembles the actual
88 stream function (contoured). The circulation changes captured by the AMOC index are thus not local
89 to the subpolar gyre region but rather represent a large scale response of the Atlantic meridional
90 overturning circulation. Despite the good correlation with the AMOC in the model, our SST-based
91 index only provides indirect evidence for possible AMOC changes.

92 **Reconstructing the AMOC index over the past millennium**

93 To obtain a long-term reconstruction of the AMOC index requires long-term reconstructions of both
94 the Northern Hemisphere mean temperature and sea surface temperature (SST) of the subpolar
95 gyre. For the Northern Hemisphere mean, Mann et al.⁹ produced reconstructions using two different

96 methods, Composite-Plus-Scale (CPS) and Errors in Variables (EIV). Here we use the land-and-ocean
97 reconstruction with the EIV method using all the available proxies, which is the reconstruction for
98 which the best validation results were achieved (see Supporting Online Material of Mann et al.⁹).
99 Based on standard validation scores (Reduction of Error and Coefficient of Efficiency), this series
100 provides a skilful reconstruction back to 900 AD and beyond (95% significance compared to a red-
101 noise null).

102 The subpolar gyre series is derived from the spatial temperature reconstruction of Mann et al.¹⁰,
103 which reconstructs land and ocean surface temperatures in every 5° latitude by 5° longitude grid box
104 with sufficient instrumental data to perform calibration and validation. The subpolar gyre falls
105 within the region where the individual grid-box reconstructions are assessed to be skilful compared
106 to a red noise null¹⁰. In addition, we performed validation testing of the subpolar gyre mean series,
107 which indicates a skilful reconstruction back to 900 AD (95% significance compared to a red-noise
108 null; see *Supplementary Information* for details).

109 Both time series as well as the resulting AMOC index are shown in Fig. 3. Remarkably, the subpolar
110 gyre reaches nearly its coldest temperatures of the last millennium in the late 20th Century (orange
111 curve), despite global warming. Mann et al.¹² already noted that this region near Greenland is
112 anomalous in being colder during the modern reference period (1961-1990) than even in the Little
113 Ice Age. The index (blue curve) shows a rather steady AMOC, with modest changes until the
114 beginning of the 20th Century. There is indication of a maximum in the 15th Century and a minimum
115 around 1600 AD. There is no sign in our index that a weak AMOC caused the 'Little Ice Age' in the
116 Northern Hemisphere¹³; rather the data are consistent with previous findings that the Little Ice Age
117 reflects a response to natural volcanic and solar forcing^{14, 15, 16}, and if anything this surface cooling
118 strengthened the AMOC at least during the first part of the Little Ice Age. The fact that LIA coldness
119 appears to have been even more pronounced in South America than in Europe¹⁷ further argues
120 against a weak AMOC, as the latter would have warmed the Southern Hemisphere. The 20th Century
121 shows a gradual decline in the AMOC index, followed by a sharp drop starting around 1970 with a
122 partial recovery after 1990 (discussed further below). This recovery is consistent with the finding of
123 an AMOC increase since 1993 based on floats and satellite altimeter data¹⁸.

124 Our temperature reconstruction for the subpolar gyre differs from three estimates based on
125 sediment cores from the region^{19,20}. However, reconciling these cores with each other and with the
126 instrumental SST record proves problematic (see *Supplementary Information*), whereas our
127 reconstruction compares well with the instrumental data during the period of overlap.

128 Spectral analysis of the AMOC index shows a few marginally significant peaks with periods around
129 22, 27 and 37 years, but these features are not clearly discernible from the expectations of simple
130 red noise (Fig. 4). We find no significant peak in the 50-70 year period range although our index
131 should pick this up¹⁰, suggesting that the “Atlantic Multidecadal Oscillation” (AMO) described by
132 Delworth and Mann and others^{21, 22, 23} is not a prominent feature of our AMOC index time series.

133 **The 20th Century AMOC weakening**

134 The most striking feature of the AMOC index is the extremely low index values reached from 1975 to
135 1995. It is primarily this negative anomaly that yields the cooling patch in the trend maps shown in
136 Fig. 1. In the following we discuss this downward spike in more detail.

137 The significance of the 1975-1995 AMOC index reduction was estimated using a Monte Carlo
138 method (see *Supplementary Information*). The annually resolved AMOC reconstruction from 900 to
139 1850 formed the basis for an ARMA(1,1) model which closely resembles the statistical properties of
140 the data. 10,000 simulated time series of the same length as the AMOC index were constructed. The
141 probability of reaching a similarly weak AMOC index as during 1975-1995 just by natural variability
142 was found to be <0.005, based on the uncertainty of the proxy data and ignoring that this weakening
143 is independently supported by instrumental data.

144 Fig. 5 shows corroborating evidence in support of a 20th Century AMOC weakening. The blue curve
145 depicts the AMOC-index shown in Fig. 3. The dark red curve shows the corresponding index based
146 on the instrumental GISS global temperature analysis. The green curve denotes oceanic nitrogen-15
147 proxy data from corals off the US north-east coast from Sherwood et al.²⁴. These annually-resolved
148 $\delta^{15}\text{N}$ data represent a tracer for water mass changes in the region, where high values are
149 characteristic of the presence of Labrador Slope Water. The time evolution of the $\delta^{15}\text{N}$ tracer agrees
150 well with that of our AMOC index (Fig. 5). Sherwood et al. report four more data points from ancient
151 corals preceding the 20th Century, the oldest one from ~500 AD. These lie all above 10.5‰, providing
152 (albeit limited) evidence that the downward excursion to values below 10‰ between 1975 and 1995
153 and the corresponding water mass change may be unprecedented in several centuries.

154 Finally Fig. 5 shows data points from repeat hydrographic sections across the Atlantic at 25° North,
155 from which Bryden et al.²⁵ originally concluded that the AMOC had slowed by 30% since the 1950s.
156 These measurements were later adjusted for seasonal variations²⁶ and are shown in this form here;
157 recent observations over 2004-2012 show inter-annual variability²⁷ with a standard deviation of 1.7
158 Sv which needs to be kept in mind.

159 **Causes of the weakening and implications for the future**

160 Since the AMOC is driven by density gradients related to deep-water formation in the high-latitude
161 North Atlantic, a weakening of the AMOC could be caused by a regional reduction in surface ocean
162 density. Curry and Mauritzen²⁸ describe an ongoing freshening trend in the northern Atlantic in
163 which the net freshwater storage has increased by 19,000 km³ between 1961 and 1995, and the
164 rapid AMOC drop in 1970 was preceded by a large-scale freshening known as the Great Salinity
165 Anomaly^{29, 30}. This freshwater anomaly was described in 1988 as “one of the most persistent and
166 extreme variations in global ocean climate yet observed in this century”³⁰, the source of which has
167 been linked to a large sea-ice export from the Arctic Ocean^{29, 30}. Dickson et al.³⁰ and Belkin et al.²⁹
168 estimate the freshwater volume anomaly of the Great Salinity Anomaly as 2,000 km³ along the
169 Labrador coast.

170 Other possible sources of freshwater addition are increasing river discharge into the Arctic Ocean³¹
171 and meltwater coming off the Greenland Ice Sheet (GIS). Since surface flow is directed northward
172 and freshwater tends to remain near the surface due to its low density, it is difficult to remove
173 freshwater from the northern Atlantic so an accumulation over longer time scales is plausible.
174 According to a recent reconstruction of the total GIS mass balance from 1840 AD³², the GIS was close
175 to balance in the 19th Century, but a major mass loss from Greenland occurred from 1900 AD to
176 1970 AD. The cumulative runoff and ice discharge anomaly (relative to the mean over 1840-1900)
177 during this period is estimated as 8,000 km³, of which 1,800 km³ was released after 1955 (Fig. 6). It is
178 thus possible that the accumulated freshwater input from Greenland may have made a significant
179 contribution to the observed freshening trend. A comparable freshening around Antarctica has
180 recently likewise been linked to ice sheet mass loss³³.

181 This dilution of the surface ocean could have weakened deep-water formation, slowing the AMOC. A
182 shutdown of deep convection in the Labrador Sea from 1969 to 1971 is well documented³⁴ and the
183 stability of Labrador Sea convection has been subject of a number of studies^{35, 36}. Perhaps as a
184 consequence of the cooling in the Greenland region starting in 1970, the GIS subsequently was
185 closer to mass balance for three decades until ~2000 AD³². Since then the GIS has started to lose
186 mass again at a rapidly increasing rate, consistent with the surface warming of the region which has
187 been attributed to a recovery of the AMOC by Robson et al.³⁷ based on model simulations initialised
188 with observations. This recovery is also seen in the AMOC index proposed in this paper.

189 Recent oceanographic measurements from the RAPID array at 26 °N in the Atlantic suggest that the
190 AMOC has been weakening again since these measurements started in 2004³⁸, although we cannot
191 conclude to what extent this temporary decrease signals an ongoing trend, and the connection
192 between subtropical and subpolar overturning especially on shorter time scales is not clear³⁹.

193 Climate models from the CMIP5 ensemble forced by natural and anthropogenic forcings generally
194 show a much weaker subpolar cooling than the observations⁶ and do not capture the observed
195 Atlantic subpolar cooling during 1970-1990, even though they show a much smaller and more short-
196 lived cooling following the Agung eruption in 1963/64⁹. The failure of the models to capture the
197 cooling is probably not due to an underestimation of the response to the Agung eruption, since
198 volcanic cooling would if anything strengthen the AMOC while the data indicate an AMOC
199 weakening⁴⁰. Rather, this failure suggests that these models either have an AMOC that is too stable
200 with respect to buoyancy forcing^{41, 42}, or are missing an important forcing (and indeed the time
201 history of Greenland meltwater runoff is not included as a forcing in the CMIP5 ensemble).

202 While major uncertainties remain about the past evolution of the AMOC for lack of direct
203 measurements, indirect evidence from various sources provides a consistent picture, linking
204 together the time evolution of temperature, ocean circulation and possibly Greenland mass balance.
205 If the interconnections between these three components continue as we have conjectured, the
206 ongoing melting of the Greenland Ice Sheet, which reached an extreme level in 2012⁴³, may lead to
207 further freshening of the subpolar Atlantic in the next few decades. Bamber et al.⁴⁴ estimate that if
208 current trends continue, the Greenland meltwater input from 1995 to 2025 AD may exceed 10,000
209 km³. This might lead to another weakening of the Atlantic overturning circulation within a decade or
210 two, and possibly even a permanent shutdown of Labrador Sea convection as a result of global
211 warming, as has been predicted by some climate model simulations^{45, 46}.

212 **Acknowledgements**

213 We thank O. Sherwood for providing coral data. MEM acknowledges support for this work from the
214 ATM program of the National Science Foundation (grant ATM-0902133). Three anonymous
215 reviewers made many suggestions that helped to improve this paper.

216 **Author contributions**

217 SRa conceived and designed the research and wrote the paper, ES, SRu, AR and GF performed the
218 research, MEM and JB contributed materials/analysis tools and co-wrote the paper.

219 **References**

- 220 1. Stouffer R, et al. Investigating the Causes of the Response of the Thermohaline Circulation to
221 Past and Future Climate Changes. *J Clim* 2006, **19**: 1365-1387.

222

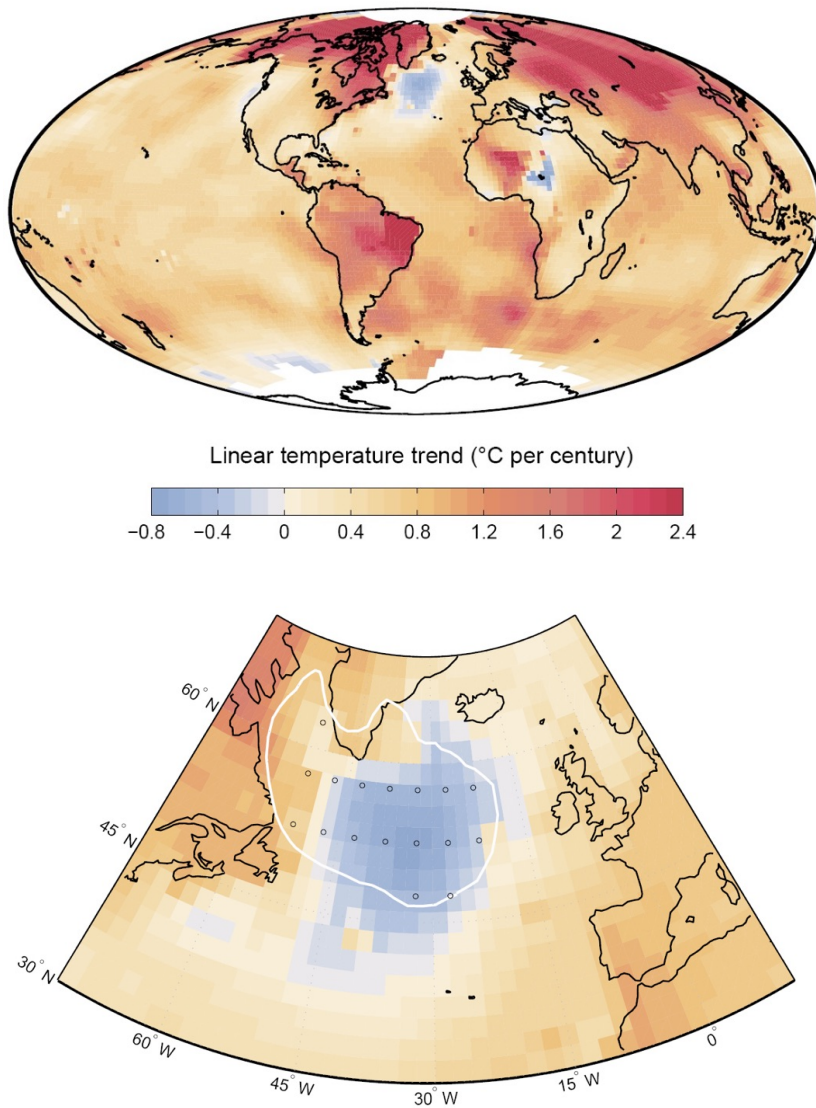
- 223 2. Latif M, Roeckner E, Botzet M, Esch M, Haak H, Hagemann S, *et al.* Reconstructing,
224 monitoring, and predicting multidecadal-scale changes in the North Atlantic thermohaline
225 circulation with sea surface temperature. *J Clim* 2004, **17**(7): 1605-1614.
- 226
- 227 3. Dima M, Lohmann G. Evidence for Two Distinct Modes of Large-Scale Ocean Circulation
228 Changes over the Last Century. *J Clim* 2010, **23**(1): 5-16.
- 229
- 230 4. Thompson DWJ, Wallace JM, Kennedy JJ, Jones PD. An abrupt drop in Northern Hemisphere
231 sea surface temperature around 1970. *Nature* 2010, **467**(7314): 444-447.
- 232
- 233 5. Feulner G, Rahmstorf S, Levermann A, Volkwardt S. On the origin of the surface air
234 temperature difference between the hemispheres in Earth's present-day climate. *J Clim*
235 2013, **26**(18): 7136-7150.
- 236
- 237 6. Drijfhout S, van Oldenborgh GJ, Cimadoribus A. Is a Decline of AMOC Causing the Warming
238 Hole above the North Atlantic in Observed and Modeled Warming Patterns? *J Clim* 2012,
239 **25**(24): 8373-8379.
- 240
- 241 7. Booth BBB, Dunstone NJ, Halloran PR, Andrews T, Bellouin N. Aerosols implicated as a prime
242 driver of twentieth-century North Atlantic climate variability. *Nature* 2012, **484**(7393): 228–
243 232.
- 244
- 245 8. Zhang R, Delworth TL, Sutton R, Hodson DLR, Dixon KW, Held IM, *et al.* Have Aerosols
246 Caused the Observed Atlantic Multidecadal Variability? *J Atmos Sci* 2013, **70**(4): 1135-1144.
- 247
- 248 9. Terray L. Evidence for multiple drivers of North Atlantic multi-decadal climate variability.
249 *Geophys Res Let* 2012, **39**.
- 250
- 251 10. Roberts CD, Garry FK, Jackson LC. A Multimodel Study of Sea Surface Temperature and
252 Subsurface Density Fingerprints of the Atlantic Meridional Overturning Circulation. *J Clim*
253 2013, **26**(22): 9155-9174.
- 254
- 255 11. Jungclaus JH, Fischer N, Haak H, Lohmann K, Marotzke J, Matei D, *et al.* Characteristics of the
256 ocean simulations in the Max Planck Institute Ocean Model (MPIOM) the ocean component
257 of the MPI-Earth system model. *Journal of Advances in Modeling Earth Systems* 2013, **5**(2):
258 422-446.
- 259
- 260 12. Mann ME, Zhang Z, Rutherford S, Bradley RS, Hughes M, Shindell D, *et al.* Global Signatures
261 and Dynamical Origins of the Little Ice Age and Medieval Climate Anomaly. *Science* 2009,
262 **326**: 1256-1260.
- 263

- 264 13. Wanamaker A, Bulter P, Scourse J, Heinemeier J, Eiríksson J, Knudsen K, *et al.* Surface
265 changes in the North Atlantic meridional overturning circulation during the last millennium.
266 *Nature Communications* 2012.
- 267
- 268 14. Crowley TJ. Causes of climate change over the past 1000 years. *Science* 2000, **289**: 270-277.
- 269
- 270 15. Shindell DT, Schmidt GA, Miller RL, Mann ME. Volcanic and solar forcing of climate change
271 during the preindustrial era. *J Clim* 2003, **16**(24): 4094-4107.
- 272
- 273 16. Feulner G. Are the most recent estimates for Maunder Minimum solar irradiance in
274 agreement with temperature reconstructions? *Geophys Res Lett* 2011, **38**.
- 275
- 276 17. PAGES 2k Network. Continental-scale temperature variability during the past two millennia.
277 *Nature Geoscience* 2013.
- 278
- 279 18. Willis J. Can in situ floats and satellite altimeters detect long-term changes in Atlantic Ocean
280 overturning? *Geophys Res Lett* 2010, **37**: L06602.
- 281
- 282 19. Moffa-Sanchez P, Born A, Hall IR, Thornalley DJR, Barker S. Solar forcing of North Atlantic
283 surface temperature and salinity over the past millennium. *Nature Geoscience* 2014, **7**(4):
284 275-278.
- 285
- 286 20. Miettinen A, Divine D, Koc N, Godtliobsen F, Hall IR. Multicentennial Variability of the Sea
287 Surface Temperature Gradient across the Subpolar North Atlantic over the Last 2.8 kyr. *J*
288 *Clim* 2012, **25**(12): 4205-4219.
- 289
- 290 21. Delworth TL, Mann ME. Observed and simulated multidecadal variability in the Northern
291 Hemisphere. *Clim Dyn* 2000, **16**(9): 661-676.
- 292
- 293 22. Chambers DP, Merrifield MA, Nerem RS. Is there a 60-year oscillation in global mean sea
294 level? *Geophys Res Lett* 2012, **39**.
- 295
- 296 23. Tung K, Zhou J. Using data to attribute episodes of warming and cooling in instrumental
297 records. *Proc Natl Acad Sci USA* 2013, **110**: 2058–2063.
- 298
- 299 24. Sherwood OA, Lehmann MF, Schubert CJ, Scott DB, McCarthy MD. Nutrient regime shift in
300 the western North Atlantic indicated by compound-specific delta N-15 of deep-sea
301 gorgonian corals. *Proceedings of the National Academy of Sciences of the United States of*
302 *America* 2011, **108**(3): 1011-1015.
- 303
- 304 25. Bryden HL, Longworth HR, Cunningham SA. Slowing of the Atlantic meridional overturning
305 circulation at 25° N. *Nature* 2005, **438**: 655-657.

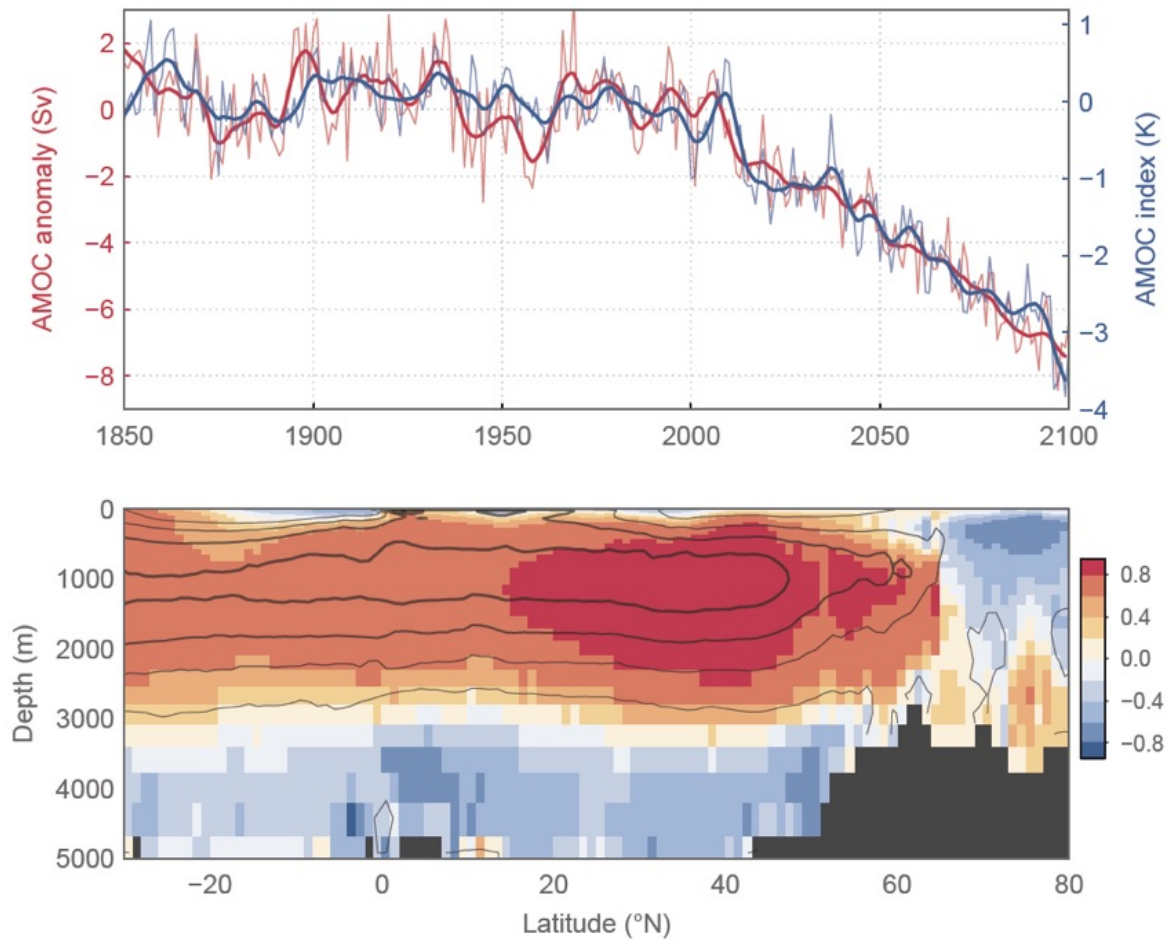
- 306
307 26. Kanzow T, Cunningham SA, Johns WE, Hirschi JJM, Marotzke J, Baringer MO, *et al.* Seasonal
308 Variability of the Atlantic Meridional Overturning Circulation at 26.5 degrees N. *J Clim* 2010,
309 **23**(21): 5678-5698.
- 310
311 27. Smeed DA, McCarthy GD, Cunningham SA, *et al.* Observed decline of the Atlantic meridional
312 overturning circulation 2004-2012. *Ocean Science* 2014, **10**: 29-38.
- 313
314 28. Curry R, Mauritzen C. Dilution of the northern North Atlantic Ocean in recent decades.
315 *Science* 2005, **308**(5729): 1772-1774.
- 316
317 29. Belkin IM, Levitus S, Antonov J, Malmberg S-A. "Great Salinity Anomalies" in the North
318 Atlantic. *Progr Oceanogr* 1998, **41**: 1-68.
- 319
320 30. Dickson RR, Meincke J, Malmberg SA, Lee AJ. The "Great Salinity Anomaly" in the northern
321 North Atlantic, 1968-82. *Progr Oceanogr* 1988, **20**: 103-151.
- 322
323 31. Peterson BJ, Holmes RM, McClelland JW, Vörösmarty CJ, Lammers RB, Shiklomanov AI, *et al.*
324 Increasing river discharge to the Arctic Ocean. *Science* 2002, **298**: 2171-2173.
- 325
326 32. Box J, Colgan W. Greenland ice sheet mass balance reconstruction. Part III: marine ice loss
327 and total mass balance (1840-2010). *J Clim* 2013, **26**: 6990-7002.
- 328
329 33. Rye C, Naveira Garabato AC, Holland P, Meredith MP, George Nurser A, Hughes CW, *et al.*
330 Rapid sea-level rise along the Antarctic margins in response to increased glacial discharge.
331 *Nature Geoscience* 2014, **7**: 732-735.
- 332
333 34. Lazier JRN. Oceanographic conditions at Ocean Weather Ship *Bravo*, 1964-74. *Atmos-Ocean*
334 1980, **18**: 227-238.
- 335
336 35. Kuhlbrodt T, Titz S, Feudel U, Rahmstorf S. A simple model of seasonal open ocean
337 convection. Part II: Labrador Sea stability and stochastic forcing. *Ocean Dyn* 2001, **52**: 36-49.
- 338
339 36. Gelderloos R, Straneo F, Katsman CA. Mechanisms behind the Temporary Shutdown of Deep
340 Convection in the Labrador Sea: Lessons from the Great Salinity Anomaly Years 1968-71. *J*
341 *Clim* 2012, **25**(19): 6743-6755.
- 342
343 37. Robson JJ, Sutton RT, Smith DM. Initialized decadal predictions of the rapid warming of the
344 North Atlantic Ocean in the mid 1990s. *Geophys Res Lett* 2012, **39**.
- 345
346 38. Robson J, Hodson D, Hawkins E, Sutton R. Atlantic overturning in decline? *Nature Geoscience*
347 2014, **7**(1): 2-3.

- 348
349 39. Lozier MS, Roussenov V, Reed MSC, Williams RG. Opposing decadal changes for the North
350 Atlantic meridional overturning circulation. *Nature Geoscience* 2010, **3**(10): 728-734.
- 351
352 40. Zhang R. Coherent surface-subsurface fingerprint of the Atlantic meridional overturning
353 circulation. *Geophys Res Lett* 2008, **35**: L20705.
- 354
355 41. Hofmann M, Rahmstorf S. On the stability of the Atlantic meridional overturning circulation.
356 *Proc Natl Acad Sci USA* 2009, **106**(49): 20584-20589.
- 357
358 42. Weaver AJ, Sedlacek J, Eby M, Alexander K, Cressin E, Fichefet T, *et al.* Stability of the
359 Atlantic meridional overturning circulation: A model intercomparison. *Geophys Res Let* 2012,
360 **39**.
- 361
362 43. Nghiem SV, Hall DK, Mote TL, Tedesco M, Albert MR, Keegan K, *et al.* The extreme melt
363 across the Greenland ice sheet in 2012. *Geophys Res Let* 2012, **39**.
- 364
365 44. Bamber J, van den Broeke M, Ettema J, Lenaerts J, Rignot E. Recent large increases in
366 freshwater fluxes from Greenland into the North Atlantic. *Geophys Res Let* 2012, **39**.
- 367
368 45. Rahmstorf S. Shifting seas in the greenhouse? *Nature* 1999, **399**: 523-524.
- 369
370 46. Wood RA, Keen AB, Mitchell JFB, Gregory JM. Changing spatial structure of the thermohaline
371 circulation in response to atmospheric CO2 forcing in a climate model. *Nature* 1999, **399**:
372 572-575.
- 373
374 47. Hansen J, Ruedy R, Glascoe J, Sato M. GISS analysis of surface temperature change. *Journal*
375 *of Geophysical Research-Atmospheres* 1999, **104**: 30997-31022.
- 376
377 48. Morice CP, Kennedy JJ, Rayner NA, Jones PD. Quantifying uncertainties in global and regional
378 temperature change using an ensemble of observational estimates: The HadCRUT4 data set.
379 *Journal of Geophysical Research-Atmospheres* 2012, **117**.
- 380
381 49. Mann ME, Lees JM. Robust estimation of background noise and signal detection in climatic
382 time series. *Clim Change* 1996, **33**(3): 409-445.

383

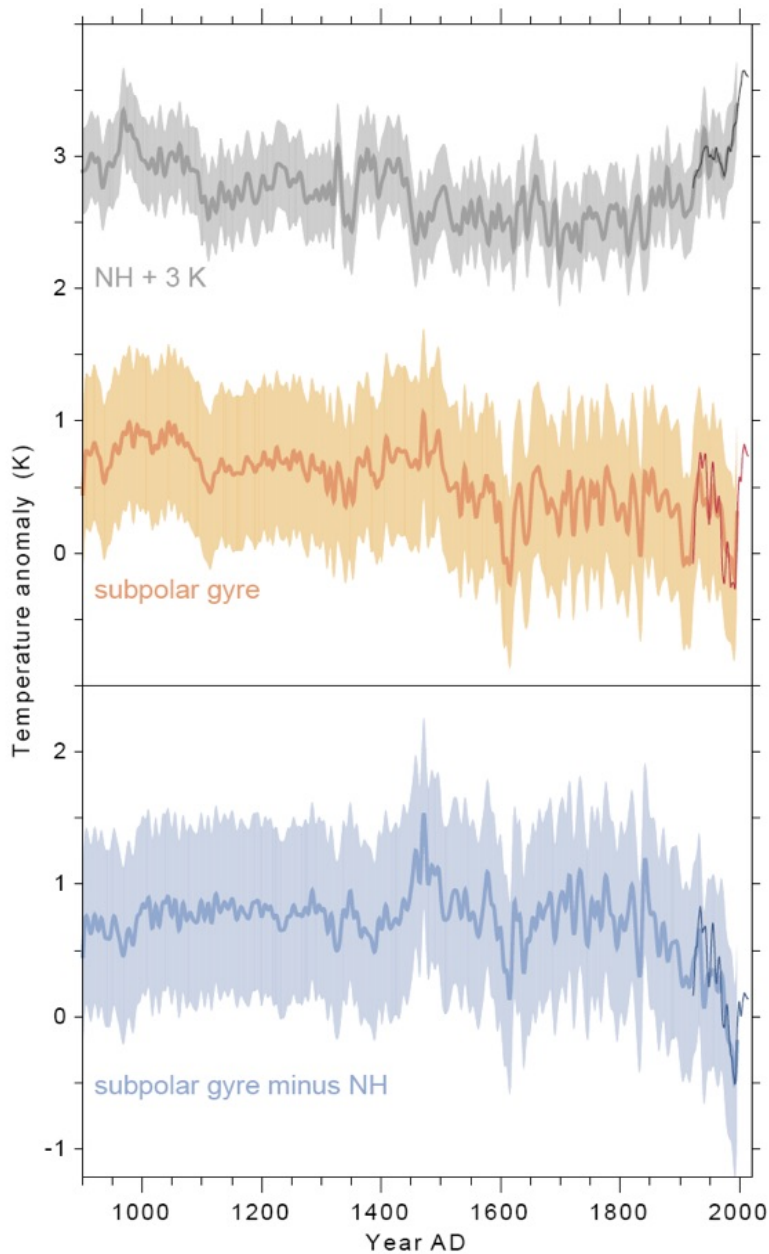


384 **Figure 1** Linear trends of surface temperature since 1901 AD based on the temperature data of
 385 NASA GISS⁴⁷, in °C per century. The upper panel is a global equal area map (Hammer projection) for
 386 1901-2013; white indicates insufficient data. In the lower panel we show the same analysis for the
 387 North Atlantic sector for 1901-2000. In addition to the observed temperature trends the lower panel
 388 also shows the grid points (black circles) of the subpolar gyre region for which time series are shown
 389 in Figs. 3 and 5, as well as the model-average 2°C cooling contour (white) from a climate model
 390 intercomparison¹ in which the models were subject to a strong AMOC reduction induced by adding a
 391 freshwater anomaly to the northern Atlantic. The geographic extent of the model-predicted
 392 temperature response to an AMOC reduction coincides well with the region of observed 20th-
 393 Century cooling. The models are forced more strongly and cooling extends further west due to
 394 shutting down Labrador Sea convection, which has only briefly happened in the real world so far.
 395 (Note that the second cooling patch in central Africa is in a region of poor data coverage and may be
 396 an artefact of data inhomogeneities.)



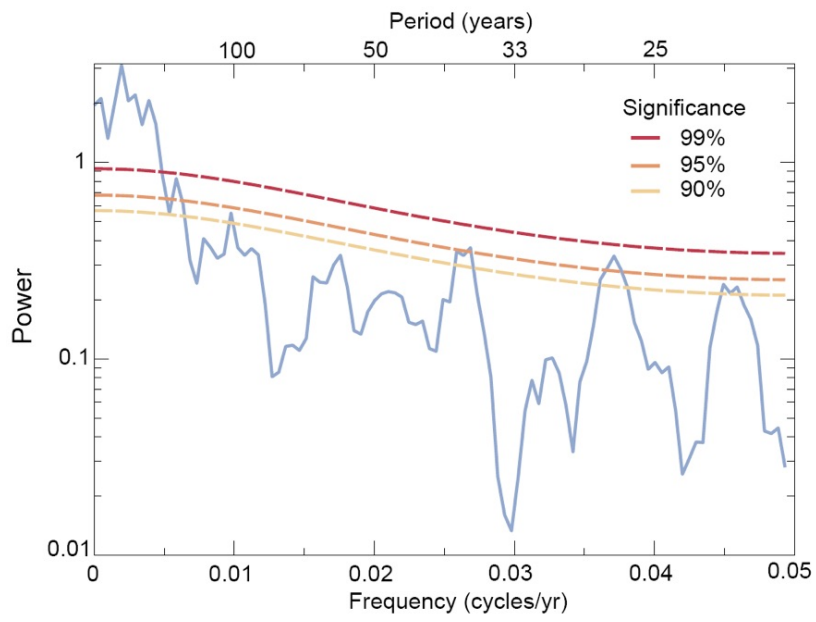
397

398 **Figure 2** Connection between the AMOC stream function and the temperature-based AMOC index in
 399 a global warming scenario (RCP8.5) simulated with the MPI-ESM-MR global climate model of the
 400 Max Planck Institute in Hamburg¹¹. **Top panel:** Time series of the maximum overturning stream
 401 function (red) and the AMOC index (blue). Thin lines show annual values, thick lines smoothed
 402 curves over 11 years. **Bottom panel:** The correlation coefficient r of the overturning stream function
 403 in the model with the AMOC index (shading), shown together with the mean stream function (black
 404 contours in 5 Sv intervals).



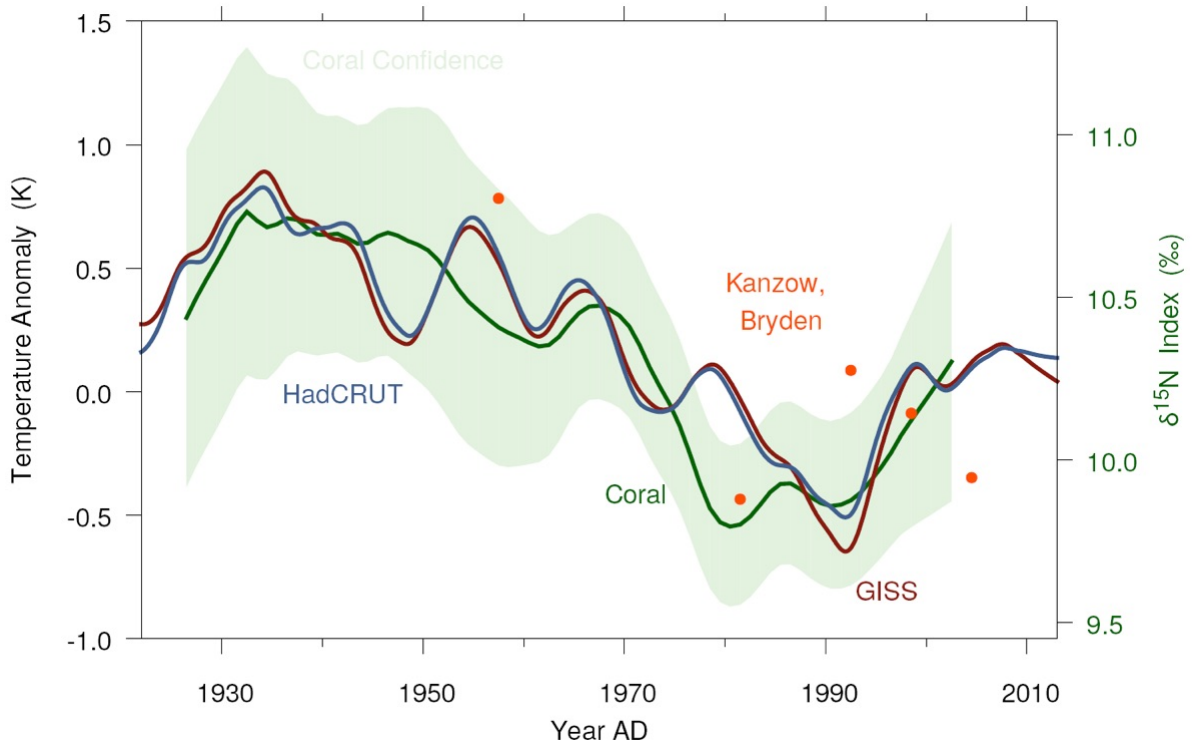
405

406 **Figure 3** Surface temperature time series for different regions from the proxy reconstruction of
 407 Mann et al.¹², including estimated 2-sigma uncertainty bands, and from the HadCRUT4 instrumental
 408 data⁴⁸. The latter are shown in darker colours and from 1922 onwards, as from this time on data
 409 from more than half of all subpolar-gyre grid cells exist in every month (except for a few months
 410 during World War II). The orange/red curves are averaged over the subpolar gyre as indicated on Fig.
 411 1. The grey/black curves are averaged over the Northern Hemisphere, offset by 3K to avoid overlap.
 412 The blue curves in the bottom panel show our AMOC index, namely the difference between subpolar
 413 gyre and Northern Hemisphere temperature anomalies (i.e. orange/red curves minus grey/black
 414 curves). Proxy and instrumental data are decadal smoothed.



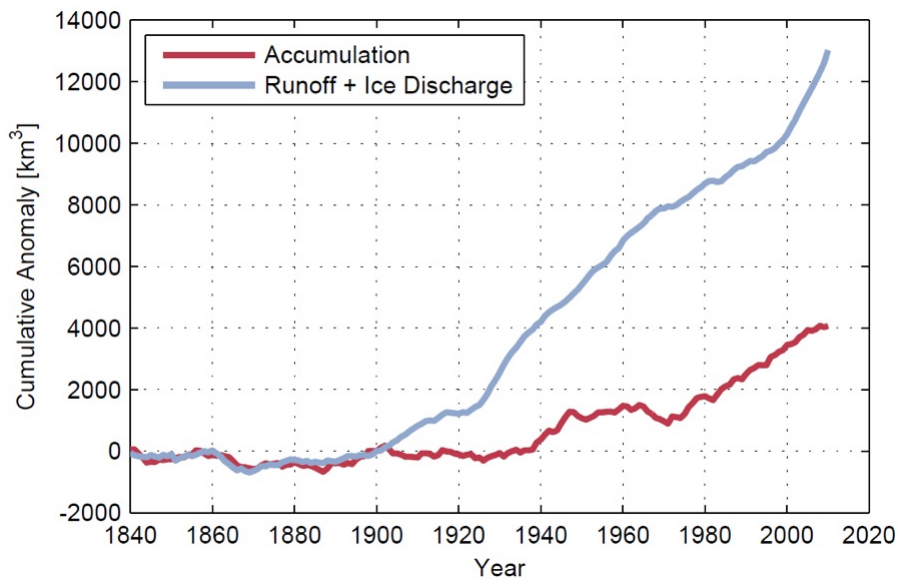
415 **Figure 4** Spectral analysis⁴⁹ of the proxy-based AMOC index shown in the bottom panel of Fig. 3.

416



417 **Figure 5** A compilation of different indicators for Atlantic ocean circulation. The blue curve shows
 418 our temperature-based AMOC index as shown in Fig. 3 (bottom panel), while the dark red curve
 419 shows the same index based on NASA GISS temperature data⁴⁷ (scale on left). The green curve with
 420 uncertainty range shows coral proxy data²⁴ (scale on right). The data are decadal smoothed.
 421 Orange dots show the analyses of data from hydrographic sections across the Atlantic at 25°N from
 422 Kanzow et al.²⁶, where a 1 K change in the AMOC index corresponds to a 2.3 Sv change in AMOC
 423 transport, as in Fig. 2 based on the model simulation.

424



425

426 **Figure 6** Mass balance terms of the Greenland Ice Sheet from Box and Colgan³². Shown is the
 427 cumulative anomaly relative to the mean over 1840-1900, a preindustrial period during which the
 428 Greenland Ice Sheet was approximately in balance.